Research and development of new neodymium laser glasses

Dongbing He[1], Shuai Kang[1,2], Liyan Zhang[1], Lin Chen[3], Yajun Ding[1,2], Qianwen Yin[1,2], and LiLi Hu[1]

[1]*Shanghai Institute of Optics and Fine Mechanics, Chinese Academy of Sciences, Shanghai 201800, China*

[2]*University of Chinese Academy of Sciences, Beijing 100049, China*

[3]*Laser Fusion Research Center, Chinese Academy of Engineering Physics, Mianyang, Sichuan 621900, China*

(Received 28 September 2016; revised 2 December 2016; accepted 12 December 2016)

Abstract

This work presents a brief introduction on three kinds of newly developed Nd^{3+}-doped laser glasses in Shanghai Institute of Optics and Fine Mechanics (SIOM), China. Two Nd^{3+}-doped phosphate glasses with lower thermal expansion coefficient and thermal shock resistance 4 times higher than that of N31 glass are developed for laser processing. Nd:Silicate and Nd:Aluminate glasses with peak emission wavelength at 1061 and 1065 nm, effective emission bandwidth of 34 and 50 nm, respectively, are developed for Exawatt-class laser system application. Fluorophosphate glasses with low nonlinear refractive index ($n_2 = 0.6$–0.86) and long fluorescence lifetime (430–$510\,\mu s$) are investigated for the purpose of decreasing B integral in high-power laser system. The properties of all these glasses are presented and compared with those of commercial neodymium laser glasses.

Keywords: aluminate glass; fluorophosphate glass; high-power laser; neodymium laser glass; phosphate glass; silicate glass

1. Introduction

Due to its good spectroscopic properties, high solubility to rare earth ions, large damage threshold and easier to be produced with large size, Nd^{3+}-doped phosphate glasses are widely used as gain media for high-peak-power lasers for inertial confinement fusion (ICF) research[1–3]. In this laser system with Million Joules energy output, laser glass must bear high energy density above 10 J cm^{-2} at 1053 nm wavelength. P_2O_5-Al_2O_3-M_2O-MO is the most suitable metaphosphate glass system till now for the application in high-peak-power laser facility, in which M_2O can be either K_2O or the mixture of alkali oxides. MO can be one of alkaline oxide or the mixture of alkaline oxides. Commercial phosphate laser glasses, such as LG-770 (from Schott of America) and LHG-8 (from Hoya of Japan), have been used in NIF (US) and LMJ (France) laser ICF facilities[4]. N31 glass developed in Shanghai Institute of Optics and Fine Mechanics (SIOM), China, has been used in Shen Guang laser facilities[5]. All these phosphate glasses have the emission cross section about $(3.6$–$3.9) \times 10^{-20}$ cm^2 and nonlinear refractive indices $(1.02$–$1.18) \times 10^{-13}$ esu. Mass production

of LHG-8, LG-770 and N31 phosphate laser glasses has been realized by continuous melting technique[5, 6].

With the development of laser technology, the application requirement is increasing in many fields, such as laser processing working at lower repetition rate, ultrafast laser system with Exawatt (simplified as EW) output, and even high-peak-power demand in ICF laser facility. The laser with 1-5Hz/50-100J output has been widely used in laser peening field[7, 8]. Glass laser with 0.1-10Hz/30-200J has been used as pump laser source for CPA or Ti: sapphire laser system to construct ultra-short Petawatt (simplified as PW) system[9–11], and hybrid glass (laser glasses with different emission bandwidths) laser was proposed as the most promising approach to realize EW laser[12]. In addition, concerning the even higher output energy requirements in high-peak-power ICF laser facility, the nonlinear optical damage will be a bottle neck to the whole laser system. Gain medium with low nonlinear refractive index n_2 is needed to decrease the B integral (a parameter that represents the cumulative nonlinear phase retardation over the optical path length)[13] in Megajoule ICF laser facility. Therefore, fluorophosphate laser glass with low n_2 was developed to meet the future development of high-peak-power laser system. On the other hand, new Nd^{3+}-doped laser glasses should be developed to meet the different requirements from the different laser applications.

Correspondence to: D. He, Shanghai Institute of Optics and Fine Mechanics, Chinese Academy of Sciences, No. 899, Huiwang Rd., Jiading, Shanghai 201800, China. Email: hdb798123@163.com

1

Table 1. Thermal–mechanical properties of silico-phosphate glasses and N31 glass.

Glass no.	Thermal conductivity (W Mk^{-1})	Fracture toughness (MPa $\times$ m1/2)	Young's modulus (GPa)	Coeff. Thermal expan. (10^{-6} K^{-1})	Thermal shock resistance (W m$^{-1/2}$)
N31	0.560	0.48	56.4	11.5	0.31
P-Si0	0.979	1.03	85.3	7.87	1.13
P-Si4	0.975	1.13	81.4	7.73	1.32
P-Si8	0.973	1.13	81.1	7.61	1.34
P-Si12	0.950	1.13	78.1	7.39	1.40
P-Si16	0.935	1.04	77.5	7.37	1.27
P-Si20	0.920	1.01	73.2	6.96	1.36

Through compositional designs and identification of special post-processing treatments, new active glasses with tailored properties have been continuously developed for specific laser architectures around the world[5, 14]. In recent years, three kinds of new Nd^{3+}-doped laser glasses have been studied and developed in SIOM, China. In this work, the compositions, main properties and applications of these neodymium laser glasses have been discussed.

2. Working principle

Phosphate glasses were prepared by conventional pot-melting technique in air atmosphere. All starting materials were introduced with high purity powder reagent. 2000 g raw materials of phosphate glass were weighted and mixed thoroughly and then melted in quartz crucibles at different temperature according to the compositions, and dehydrated with O_2 or N_2, and then poured into an airtight platinum crucible for refining and stirring. Afterward the melts were casted onto a preheated steel plate and annealed in a furnace around the glass transition temperatures and cooled gradually to room temperature. Similarly, fluorophosphate glasses were prepared in airtight platinum too, but the humidity of atmosphere should be controlled in the melting process. All samples were cut and polished carefully with the size of 25 mm $\times$ 15 mm $\times$ 5 mm for optical property measurements.

The densities were measured through the Archimedes method using distilled water as an immersion liquid, and refractive indices were achieved by the prism minimum deviation method. The absorption spectra were recorded with a PerkinElmer Lambda 900 UV/VIS/NIR spectrophotometer in the range of 200–1000 nm, while the emission spectra were obtained with a Triax 320 type spectrometer in the range of 1000–1200 nm excited at 808 nm by Xenon lamp. All measurements were carried out at room temperature. The thermo-optic parameters were determined using Mach–Zehnder interferometer with a 632.8 nm He–Ne laser on glass samples sized $\varphi6 \times 50$ mm. The stimulated emission cross section (σ_{em}) and radiative lifetime for the $^4F_{3/2} \rightarrow$ $^4I_{11/2}$ transition are calculated by the J–O theory based on measured refractive index of glass, ion concentration of rare earth ions as well as absorption and fluorescence spectra[15].

3. Silico-phosphate neodymium laser glasses with high thermal shock resistance

Nd:phosphate glass with high thermal shock resistance is usually used in high-average-power laser system. Typical application is laser peening processing. Figure of merit of high-average-power Nd:phosphate glass is shown in

$$FOM_{tm} = \frac{\sigma_{\max} K (1 - v)}{\alpha E}, \quad (1)$$

$$\sigma_{\max} = \frac{K_{Ic}}{\sqrt{a}}, \quad (2)$$

where E is Young's modulus, $\sigma_{\max}$ is fracture strength, K is thermal conductivity, v is Poson's ratio. α is linear thermal expansion coefficient. K_{Ic} is the fracture toughness, a is the flaw depth in glass.

For applications in high-average-power laser, the Nd:phosphate glass works in lower repetition rate, such as 0.1–15 Hz, then a high thermal shock resistance is needed. According to Equation (1), the solution is to maximize the thermal conductivity and fracture toughness, minimize the coefficient of thermal expansion and Young's modulus. On the other hand, emission cross section should be optimized to ensure the gain property. In addition, glass should have low temperature coefficient of the optical path length to reduce the thermal distortion effect in Nd:glass in repetition case. Consequently, considerable efforts have been done on optimizing the glass compositions of this kind of Nd:glass[16, 17].

In order to increase the thermal conductivity and reduce the thermal expansion coefficient, phosphate glass system, P_2O_5-Li_2O-MgO-Al_2O_3-SiO_2, was chosen. Six kinds of $(65-x)$ P_2O_5-$x$$SiO_2-15Al_2O_3-10Li_2O$-10MgO glasses ($x =$ 0, 4, 8, 12, 16, 20 mol%) with different combinations of P_2O_5 and SiO_2 were designed to achieve high thermal shock resistance and modest laser properties, and designated as P-Si0, P-Si4, P-Si8, P-Si12, P-Si16 and P-Si20. Table 1 shows their thermal shock properties, and as a reference, the corresponding properties of N31 glass are also given. It is known that through composition optimization, thermal conductivity can be improved by 2 times and the thermal expansion coefficient decreased to 1/2, and then the thermal

Table 2. Emission cross section and thermal–optical properties of Nd^{3+}-doped P_2O_5-Al_2O_3-BaO-K_2O-Li_2O phosphate glass.

Mol%	Coeff. of thermal expan. $(10^{-6} \, K^{-1})$	Temperature coeff. of refractive index $(10^{-6} \, K^{-1}, 50{-}100\,°C)$	Thermo-optical coeff. $(10^{-6} \, K^{-1}, 50{-}100\,°C)$	Emission cross section $(10^{-20} \, cm^2)$
Ba-Li0	92	−13	3.8	3.50
Ba-Li6	88	−15.6	3.3	3.41
Ba-Li11	90	−16.6	3.3	3.25
Ba-Li16	94	−25.5	2.7	3.13
K-Li0	105	−34.4	2.1	4.10
K-Li3	112	−46.9	1.3	4.32
K-Li6	115	−54.4	0.7	4.22
K-Li9	110	−46.8	1.1	4.36
K-Li12	115	−47.5	0.9	4.52
K-Li15	133	−85.0	−1.5	4.30

shock resistance was improved 4 times compared with that of N31 glass.

In phosphate laser glass, the thermal–optical properties were also studied by adjusting the content of alkali oxides and alkaline oxides. Table 2 shows the emission cross section and thermal–optical properties of P_2O_5-Al_2O_3-BaO-Li_2O phosphate glass. In $(60{-}70)P_2O_5$-$(7{-}10)Al_2O_3$-$(22{-}x)BaO$-xLi_2O ($x = 0, 6, 11, 16$) glass system, the thermal–optical coefficient can be reduced from 3.8×10^{-6} to $2.7 \times 10^{-6} \, K^{-1}$ with little effect on thermal expansion coefficient, just by the substitution of Ba^{2+} for Li^+, which were marked as Ba-Li0, Ba-Li6, Ba-Li11 and Ba-Li16.

$(60{-}65)P_2O_5$-$(3{-}7)Al_2O_3$-$(10{-}18)BaO$-xK_2O-$(15{-}x)Li_2O$ series glasses ($x = 0, 3, 6, 9, 12, 15$), which were labeled as K-Li0, K-Li3, K-Li6, K-Li9, K-Li12 and K-Li15, the replacement of Li^+ by K^+ was also studied. It can be found that the thermo-optical coefficient can be obviously reduced to zero and even negative (can obtain the athermal laser glass further), which benefits to compensate the laser beam distortion caused by thermal lens effect[18]. In addition, it can be seen that the stimulated emission cross section can be improved from 4.1×10^{-20} to $4.5 \times 10^{-20} \, cm^2$.

Based on the previous studies, two kinds of high-average-power Nd:phosphate glasses, NAP-2 and NAP-4, are developed in SIOM. Glass composition design, pot-melting technology, surface etching processing and thermal shock resistance of NAP-2 glass have been systematically investigated[16, 17]. The main properties of NAP-2 and NAP-4 from SIOM with those of HAP-4 (Hoya), APG-1 and APG-2 (Schott) glasses are given in Table 3. Comparing the data in Tables 1 and 2, it is found that the thermal conductivity and the thermal expansion coefficient of NAP-2 are equivalent with those of APG-1, while the temperature coefficient of the optical path length of NAP-2 is smaller than those of HAP-4 and APG-1, which is helpful to decrease the thermal lens effect of laser beam for the applications in repetition-rate laser.

Table 3. Main parameters of high-average-power neodymium phosphate laser glasses from Hoya[3], Schott[3] and SIOM.

Parameters	HAP-4	APG-1	APG-2	NAP-2	NAP-4
$\sigma_{emi}/10^{-20} \, cm^2$	3.6	3.4	2.4	3.7	3.2
$\tau_{rad}/\mu s$	350	385	464	380	400
$\Delta\lambda_{eff}/nm$	27.0	27.8	31.5	27.0	29.0
* $d/g/cm^2$	2.70	2.64	2.56	2.76	2.60
* n_d	1.5433	1.5370	1.5127	1.542	1.530
$n_{1053 \, nm}$	1.5331	1.5260	1.5032	1.536	1.523
Abbe number	64.6	67.7	66.9	67	66
$n_2/10^{-13}$ esu	1.21	1.13	1.06	1.22	1.10
$T_g/°C$	486	450	549	478	545
$\alpha/10^{-7}/K(20{-}300\,°C)$	72	99.6	64	96	71
$dn/dT/10^{-7}/K$	18	12	34	−8.7	19
$dS/dT/10^{-7}/K$	57	52	76	36	50
$k/W/(m\cdot K)$	1.02	0.78	0.84	0.76	0.86
E/GPa	70	71.0	64.0	58	67

* Parameters which may vary with the Nd_2O_3 concentration in glass.

4. Silicate and aluminate neodymium laser glasses with ultra-broad emission bandwidth

The Texas Petawatt Laser has proved that it is possible to combine two laser glasses with different gain spectra together to create laser power exceeding the world's largest Ti:Sapphire systems at a fraction of the cost[12]. While this technology is a proved route to high-power, compressed-pulse PW lasers, but the emission bandwidth of laser glasses had limited the further scaling to EW level[19].

Laser glasses used in PW systems must meet two conflicting requirements: broad emission bandwidth and low saturation fluence. PW lasers require gain media with broad spectral bandwidth ($\Delta\upsilon$) to accommodate the short pulse width. This limitation is generally expressed by the product of pulse-length (t_p) times bandwidth ($\Delta\upsilon$), which for a chirped Gaussian-shape pulse is[1]:
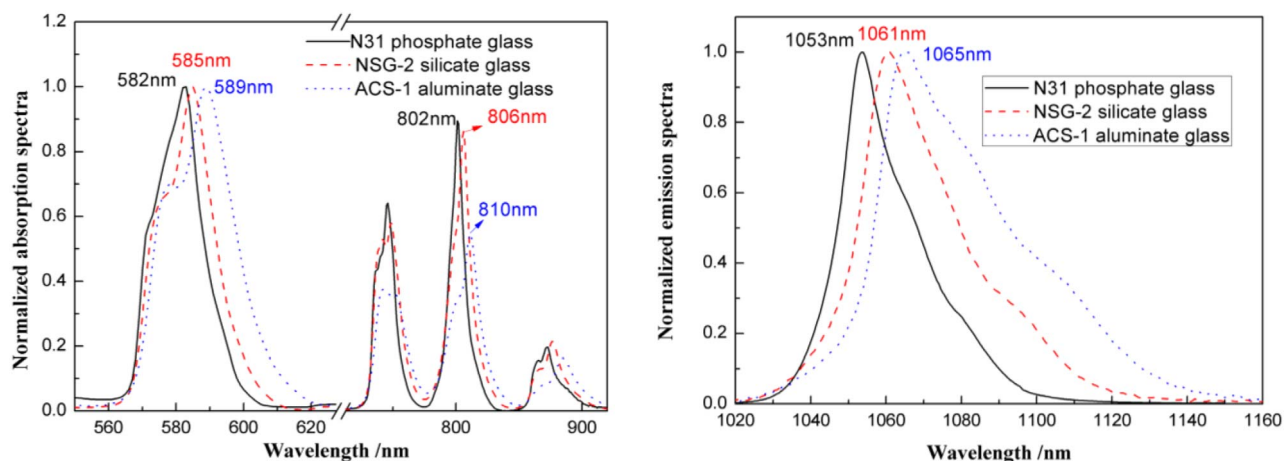
$$t_p \Delta\upsilon \sim 0.5. \tag{3}$$

Figure 1. The absorption (left) and emission (right) spectrum of phosphate, silicate and aluminate glass.

Table 4. Range of optical parameters of Nd^{3+} in different host glasses[21].

Parameters	Refractive index n_{1064}	Peak wavelength λ (nm)	Line width FWMH (nm)	Emission cross section σ_{emi} $(10^{-20} \ cm^2)$	Radiative lifetime τ_{rad} (μs)
Silicate	1.46–1.75	1057–1088	34–55	0.9–3.6	170–1090
Germinate	1.61–1.71	1060–1063	36–43	1.7–2.5	300–460
Phosphate	1.49–1.63	1052–1057	22–35	2.0–4.8	280–530
Aluminate	1.64–1.77	1063–1077	33–44	1.5–2.1	270–410

Therefore, laser glasses used to amplify very short temporal pulse must have broad gain (or emission) bandwidths. For CPA systems, the merit function of laser glass selection should shift from emission cross section and low nonlinear coefficient parameters to a broader gain spectrum[20]. Table 4 summarizes the spectroscopic properties in different host glasses[21]. From a knowledge of emission bandwidth, neodymium-doped silicate, germanate and aluminate glass are suitable to meet these needs. In the investigations of Texas Petawatt Laser, two kinds of laser glasses have been identified specially from nearly 250 glass compositions due to their significantly broader spectrum. These two glasses are designated as K-824 Nd:Ta-Silicate and L-65 Nd:Aluminate glass. However, neither of them was commercially available because of the serious crystallization problem during fabrication process[19, 22].

In CaO-BaO-Al_2O_3 glass, the effects of SiO_2 and Ga_2O_3 on the spectra properties have been studied[23]. The spectroscopic properties of ACS (Al_2O_3-CaO-BaO-SiO_2) and ACG (Al_2O_3-CaO-BaO-Ga_2O_3) glasses have been given in Table 5. The ACS series glasses have relatively broader bandwidth and long fluorescent lifetime, and the ACG glass has better glass-forming and fabrication properties.

In SIOM, NSG-2 silicate glass and ACS-1 aluminate glass with broadband emission spectra have been developed. The main parameters of these two laser glasses were given in Table 6 and compared with those of LG-680 from Schott,

Table 5. Bandwidth and Emission cross section of Nd^{3+}-doped aluminate glasses.

Glass	Line width FWMH (nm)	Effective bandwidth $\Delta\lambda_{eff}$ (nm)	Radiative lifetime τ_{rad} (μs)	Emission cross section σ_{emi} $(10^{-20} \ cm^2)$
ACS-1	41.2	49.9	338	1.84
ACS-2	38.4	47.9	335	1.90
ACS-3	37.1	46.4	343	1.92
ACS-4	36.3	44.7	341	2.02
ACG-1	38.8	48.3	311	1.75
ACG-2	38.5	47.3	305	1.84
ACG-3	38.8	47.9	293	1.89
ACG-4	38.1	46.8	275	2.0

K-824 Nd:Ta-silicate, L-65 Nd:aluminate glass from LLNL reports[19]. Fluorescence peak wavelengths of these glass locate at wavelength larger than 1060 nm, which is red shifted from the Nd:phosphate glass peaked at 1053 nm, and this feature will benefit the broadening of gain bandwidth to support the shorter pluses of hybrid glass laser system. Figure 1 shows the absorption and emission spectra of Nd^{3+}-doped phosphate, silicate and aluminate glasses. It indicates that emission peak wavelengths of Nd^{3+} ions at three different glasses change within 8–12 nm range, which provides the laser glass a solution to the mixed glass technique for EW laser system.

Table 6. Main parameters of laser glasses from Schott, LLNL and SIOM.

Parameters	LG-680	K-824	L-65	NSG-2	ACS-1
λ_p	1061	1064.5	1067	1061	1065
$\sigma/10^{-20}$ cm^2	2.7	2.4	1.8	2.9	1.84
τ_{rad}/μs	359	274	349	330	338
FWMH/nm	27.8	38.2	41.23	28	41.2
$\Delta\lambda_{eff}$/nm	34.4	42.64	—	35	49.9

Table 7. Emission cross section and nonlinear refractive index in commercial silica/silicate and FP glasses.

Glass code	$\sigma_{emi}/10^{-20}$ cm^2	$n_2/10^{-13}$ esu	Glass type
Nd-SG	1.4	0.87	Silica
LG-670(ED-2)	2.7	1.41	Silicate
LG-680(ED-3)	2.5	1.60	Silicate
Q246	2.4	1.49	Silicate
K-824	2.4	3.44	Silicate
LG810	2.54	0.52	Fluorophosphate
LHG10	2.6	0.61	Fluorophosphate

5. Fluorophosphate glass with low nonlinear refractive index

Concerning of the much higher laser energy demanded in ICF laser facility, the risk of nonlinear optical damage will increase. B integral[13], which is closely related to nonlinear refractive index, should be controlled to be as lower as possible. Intensity ripples (noise) that occur at certain spatial frequencies grow exponentially with B. B integral is calculated according to the equation[24]:

$$\boldsymbol{B}(z,t) = \frac{2\pi}{\lambda} \int_0^l n_2 \boldsymbol{I}(0,t)\,\mathrm{d}z, \qquad (4)$$

where $I(0,t)$ is the intensity of the incident light, z is the propagation distance of laser, l is length of the gain medium, and λ is the incident light wavelength), n_2 is the nonlinear refractive index. The gain medium with low n_2 is needed in order to decrease the B integral. Compared with other laser glass systems, fluorophosphate glass is a special one that combines the advantages of fluorides and phosphate glasses: higher thermal and chemical stability than fluoride glass; higher OH$^-$ resistance ability than phosphate glass; athermal behavior, low refractive index; low dispersion, and most importantly, low nonlinear refractive indices; long fluorescence lifetime and tailorable properties by varying the F/P ratio[25, 26]. Table 7 gives the n_2 and σ_{emi} data of Nd^{3+}-doped silica/silicate and FP glasses, in which LG810 (from Schott) and LHG10 (from Hoya) are Nd^{3+}-doped fluorophosphate glasses with obviously lower n_2 compared with other Nd^{3+}- doped glasses.

Two kinds of Nd^{3+}:fluorophosphate glasses with small n_2 have been developed in SIOM. NF-1 focuses on low n_2 and NF-2 aims to achieve higher emission cross section and better thermal–mechanical properties. Both glasses are with low phosphate content and fluoride alkalis free to maintain lower n_2 but higher glass transition temperature. The base glass composition is (5-13 mol%) phosphates-(15-27) AlF$_3$-(7-11) MgF$_2$-(15-24) CaF$_2$-(8-16) SrF$_2$-(8-12) BaF$_2$-(0-5) YF$_3$. Both NF glasses perform good glass-forming ability and higher thermal stability as well as large $\Delta\lambda_{eff}$ value because of the inhomogeneous broadening feature of the mixed glass formers in this kind of glass. Table 8 shows properties of Nd^{3+}: fluorophosphate glasses from Schott (LG810) Hoya (LHG10) and SIOM (NF-1 and NF-2). Lifetime of NF-1 can keep 335 μs when Nd$_2$O$_3$wt% is 2.8%.

A simulation base on the conditions of ΔB (rad) $\leqslant$ 1.8 (ΔB is the B integral accumulated by the beam passing between two pinholes)[27] and ΣB (rad) $\leqslant$ 3.5 (ΣB is the B integral for the entire chain from beam injection to the input of frequency converter)[28] has been carried out to evaluate the contribution of Nd^{3+}-doped fluorophosphate glass to the maximum output energy of a laser system with different combinations of N31 and NF-1 glasses. The restrictive conditions that ΔB (rad) $\leqslant$ 1.8 and ΣB (rad) $\leqslant$ 3.5 were set to maintain a better beam quality. The stimulated emission cross section of N31 glass is 3.8×10^{-20} cm^2, and n_2 of N31 glass is 1.18×10^{-13} esu^5. Table 9 shows

Table 8. Properties of Nd^{3+}-doped fluorophosphate glasses from Schott, Hoya and SIOM.

Properties	LG810 Schott	LHG10 Hoya	NF-1 SIOM	NF-2 SIOM
Emission cross section σ_{emi} (10^{-20} cm^2)	2.54	2.6	2.7	3.4
Nd$_2$O$_3$wt%	1.2	2.4	0.5	0.5
Fluorescent lifetime (μs)	470	384	510	430
Lasing wavelength λ_L (nm)	1053	1051	1053	1052
Effective line width $\Delta\lambda_{eff}$ (nm)	—	—	32.8	30.4
n_d	1.434	—	1.4647	1.5146
Abbe Number	91	—	88	77
Nonlinear refractive index, n_2 (10^{-13}esu)	0.52	0.61	0.6	0.86
Glass transition temperature (°C)	395	—	450	490
dn/dT (10^{-6}/K)	—	—	−8.8	−8.6
dS/dT (10^{-6}/K)	−1.4	1.6	−1.86	−1.2
α (30–300 °C) (10^{-7}/K)	—	—	152	142

Table 9. Simulation results with total 18 pieces of NF-1 and N31 glass slabs, pulse width 5 ns.

$Gain_{N31}$ (%cm^{-1})	$Gain_{NF-1}$ (%cm^{-1})	Nd:glass combination	ΔB (rad)	ΣB (rad)	Input (J)	Output (J)
5.25	/	$9_{(N31)} + 9_{(N31)}$	1.79	2.60	0.016	16 870
5.25	4.36	$9_{(N31)} + 9_{(NF-1)}$	1.80	3.12	0.076	21 398
5.25	4.36	$9_{(N31)} + 1_{(N31)} + 8_{(NF-1)}$	1.80	3.07	0.065	21 089
5.25	4.36	$9_{(N31)} + 3_{(N31)} + 6_{(NF-1)}$	1.78	2.91	0.045	20 056
5.25	4.36	$9_{(N31)} + 5_{(N31)} + 4_{(NF-1)}$	1.78	2.79	0.032	19 087
5.25	4.36	$9_{(N31)} + 7_{(N31)} + 2_{(NF-1)}$	1.79	2.70	0.023	18 102
Output energy performs 7–27% enhancement						

the simulation results. The replacement of NF-1 glass to N31 glass showed that the output energy improves 7%–27% with the contribution of small n_2 of NF-1 glass.

6. Conclusion

Three kinds of neodymium laser glasses have been developed in SIOM, China. In phosphate laser glass, the thermal shock resistance, emission cross section and thermal–optical properties were studied and NAP-2 and NAP-4 glasses with improved thermal–mechanical properties and suitable laser properties were developed for high-average-power laser system. The Nd^{3+}-doped silicate (NSG-2) and aluminate (ACS-1) glasses with broad effective emission bandwidth of 34 and 50 nm, respectively, having potential applications in the EW-class laser facility, have been developed. The properties of two kinds of Nd^{3+}-doped fluorophosphate glasses (NF-1 and NF-2) with low nonlinear refractive index ($n_2 = 0.6$–0.86) and long fluorescence lifetime (430–510 µs) were presented, and simulation work showed that the replacement of NF-1 glass to N31 glass in high-power laser device results in 7%–27% improvement of output energy.

References

1. J. H. Campbell, J. S. Hayden, and A. Marker, Int. J. Appl. Glass Sci. **2**, 3 (2011).
2. C. Danson, D. Hillier, N. Hopps, and D. Neely, High Power Laser Sci. Engng **3**, e3 (2015).
3. J. H. Campbell and T. I. Suratwala, J. Non-Cryst. Solids **263–264**, 318 (2000).
4. V. Arbuzov, Y. K. Fyodorov, S. Kramarev, S. Lunter, S. Nikitina, A. Pozharskii, A. Shashkin, A. Semyonov, V. Ter-Nersesyants, A. Charukhchev, V. Sirazetdinov, S. Garanin, and S. Sukharev, Glass Technol. **46**, 67 (2005).
5. L. Hu, S. Chen, J. Tang, B. Wang, T. Meng, W. Chen, L. Wen, J. Hu, S. Li, Y. Xu, Y. Jiang, J. Zhang, and Z. Jiang, High Power Laser Sci. Engng **2**, e1 (2014).
6. J. H. Campbell, T. I. Suratwala, C. B. Thorsness, J. S. Hayden, A. J. Thorne, J. M. Cimino, A. J. Marker, III, K. Takeuchi, M. Smolley, and G. F. Ficini-Dorn, J. Non-Cryst. Solids **263–264**, 342 (2000).
7. C. B. Dane, L. A. Hackel, J. Daly, and J. Harrisson, Mater. Manuf. Processes **15**, 81 (2000).
8. C. B. Dane, L. A. Hackel, J. M. Halpin, J. Daly, J. Harrisson, and F. Harris, SPIE **3887**, 211 (2000).
9. A. A. Kuzmin, O. V. Kulagin, E. A. Khazanov, and A. A. Shaykin, Quantum Electron. **43**, 597 (2013).
10. T. Sekine, Y. Takeuchi, and T. Kawashima, J. Phys.: Conf. Ser. **688**, 012104 (2016).
11. J. P. Zou, C. Le Blanc, D. N. Papadopoulos, G. Chériaux, P. Georges, G. Mennerat, F. Druon, L. Lecherbourg, A. Pellegrina, P. Ramirez, F. Giambruno, A. Fréneaux, F. Leconte, D. Badarau, J. M. Boudenne, D. Fournet, T. Valloton, J. L. Paillard, J. L. Veray, M. Pina, P. Monot, J. P. Chambaret, P. Martin, F. Mathieu, P. Audebert, and F. Amiranoff, High Power Laser Sci. Engng **3**, e2 (2015).
12. E. W. Gaul, M. Martinez, J. Blakeney, A. Jochmann, M. Ringuette, D. Hammond, T. Borger, R. Escamilla, S. Douglas, W. Henderson, G. Dyer, A. Erlandson, R. Cross, J. Caird, C. Ebbers, and T. Ditmire, Appl. Opt. **49**, 1676 (2010).
13. S.-c. Wen and D.-y. Fan, Acta Opt. Sin. **21**, 1331 (2001).
14. J. S. Hayden, Int. J. Appl. Glass Sci. **6**, 19 (2015).
15. B. R. Judd, Phys. Rev. **127**, 504 (1962).
16. H. Chen, D. He, L. Hu, S. Li, and J. Cheng, Chin. J. Lasers **37**, 2035 (2010).
17. W. Li, D. He, S. Li, W. Chen, and L. Hu, Ceram. Int. **40**, 13389 (2014).
18. S. M. Jackel, A. Kaufman, and R. Lallouz, Opt. Eng. **33**, 3008 (1994).
19. G. R. Hays, E. W. Gaul, M. D. Martinez, and T. Ditmire, Appl. Opt. **46**, 4813 (2007).
20. E. W. Gaul, G. R. Hays, M. D. Martinez, and T. Ditmire, in *Frontiers in Optics* (2005), paper JTuF3.
21. M. J. Weber, J. Non-Cryst. Solids **123**, 208 (1990).
22. M. L. Baesso, A. C. Bento, L. C. M. Miranda, D. F. de Souza, J. A. Sampaio, and L. A. O. Nunes, J. Non-Cryst. Solids **276**, 8 (2000).
23. S. Kang, D.-B. He, S. Gao, F.-F. Huang, Y.-J. Ding, and L.-L. Hu, J. Inorganic Materials **30**, 1177 (2015).
24. M. Shao, H.-W. Fu, Z.-Q. Lin, and X.-G. Qiao, High Power Laser Part. Beams **21**, 1776 (2009).
25. F. X. Gan, *Optical Glasses* (Science Publishing Company, Beijing, 1964), p. 260.
26. L. Y. Zhang, L. L. Hu, and Z. H. Jiang, Tunable Fiber Lasers **23**, 474 (2003).
27. J. Yang, X. M. Zhang, D. X. Hu, W. Y. Wang, and J. Q. Su, Opt. Laser Technol. **39**, 123 (2007).
28. F. Wang, J. Su, and W. Wang, Chin. Opt. Lett. **5**, s190 (2007).